Department of Pesticide Regulation

Mary-Ann Warmerdam
Director

M E M O R A N D U M

Arnold Schwarzenegger
Governor

TO: Randy Segawa
Environmental Program Manager I
Environmental Monitoring Branch

FROM: Frank Spurlock, Research Scientist III *Original signed by*
Environmental Monitoring Branch
916-324-4124

Rick Bergin, Environmental Scientist *Original signed by*
Environmental Monitoring Branch

Atac Tuli, Environmental Scientist *Original signed by*
Environmental Monitoring Branch

Bruce Johnson, Research Scientist III *Original signed by*
Environmental Monitoring Branch

DATE: May 6, 2010

SUBJECT: FUMIGANT TRANSPORT MODELING USING HYDRUS: 4. DEVELOPMENT AND TESTING OF MODIFICATIONS TO ENHANCE FUMIGANT FIELD SIMULATIONS

ABSTRACT

Several modifications to the HYDRUS1D and HYDRUS2/3D models were proposed by Department of Pesticide Regulation's (DPR's) Air and Ground Water Groups to enhance simulation of fumigant vadose zone transport. The modifications were implemented by the models' primary author, Dr. Jirka Šimůnek, and included various changes to input/output data and file formats, temperature dependence of the stagnant surface boundary layer, ability to simulate tarp removal mid-simulation, ability to simulate incorporated applications mid-simulation, and implementation of dual volatilization boundary conditions at the soil surface. The specific modifications and DPR's subsequent testing of their computational integrity are documented in this report. In summary, while a few programming errors were initially found and repaired, the testing results reported herein for the final modification versions indicate the modified code works as expected and contains no known errors. The very small deviations between the unmodified and modified model versions observed in some cases were attributable to numerical error as is common with finite element models.

I. INTRODUCTION

DPR has been evaluating the use of HYDRUS1D and HYDRUS2/3D models (Šimůnek et al., 2006; Šimůnek et al. 2009) for simulating post-application fumigant volatilization from soils. Previous DPR reports have investigated potential errors in simulated volatilization arising from use of inaccurate pedotransfer functions to estimate soil hydraulic parameters (Spurlock, 2008), evaluated HYDRUS1D and HYDRUS2/3D numerical algorithms for both the gas phase diffusion/sorption process within soil and first-order mass transfer surface volatilization process at the soil surface (Spurlock, 2009), and conducted sensitivity analysis of model outputs to fumigant physical-chemical properties (Spurlock, 2010).

The HYDRUS models have been widely used for simulating a variety of vadose zone transport problems (<http://www.pc-progress.com/en/Default.aspx?h3d-references>). However, there are unique aspects to simulating post-application fumigant volatilization as compared to other types of transport problems. For example, in California many fumigant/application method combinations require use of a plastic film over the soil ("tarp") for a specified period after application. In the HYDRUS models, a tarp is simulated using a stagnant boundary layer at the soil surface. The thickness of the boundary layer is chosen to provide a mass transfer resistance at the soil surface equivalent to that of tarp (Spurlock, 2010). However, tarp permeabilities to fumigants are often highly temperature dependent (Paperniek, 2006), in part contributing to diurnal increases and decreases in fumigant flux. The current versions of HYDRUS1D and HYDRUS2/3D do not have the capability to simulate this temperature dependence. This limits their ability to accurately simulate fumigant diurnal flux dynamics. To address this and other limitations, DPR contracted with the primary HYDRUS developer, Dr. Jirka Šimůnek, to implement several modifications to the current HYDRUS models, thereby improving their ability to simulate fumigant volatilization from soils. These included:

1. *Modification*: Simulation of temperature-dependent variable boundary layer thickness. The temperature dependence is described using an Arrhenius-type relationship similar to other HYDRUS temperature-dependent variables. *Purpose*: To allow simulation of temperature dependent tarp permeability. *Programs*: HYDRUS1-D and HYDRUS2/3D

2. *Modification*: Automatically create text output file of nodal total, dissolved, solid, and gas phase concentrations; and water content and temperature. *Purpose*: To allow more convenient inverse parameter estimation using 3rd party software such as PEST (<http://www.pesthomepage.org/Home.php>). PEST is a flexible nonlinear parameter estimation program, and also has the ability to allow Monte Carlo simulations. *Programs*: HYDRUS1-D and HYDRUS2/3D.

3. *Modification*: Specification of Total (dissolved plus sorbed plus gas-phase) initial nodal concentrations as opposed to only dissolved concentration as in current HYDRUS programs. *Purpose*: Provides a much more convenient method of specifying initial conditions. *Program*: HYDRUS2/3D.

4. *Modification*: Include the ability to model mid-simulation incorporated pesticide applications. This might include, for instance, soil incorporation of an herbicide (0–7.5 cm) or broadcast injection of a fumigant (depth 30–45 cm). *Purpose*: This capability is needed by DPR's ground water group for certain modeling scenarios. *Programs*: HYDRUS1-D and HYDRUS2/3D.

5. *Modification*: Include the Moldrup Water Linear Reduction Model (WLR) as an option for describing the effects of gas-phase tortuosity on diffusion. *Purpose:* This modification provides the more recent WLR model as an alternative to the conventional Millington-Quirk tortuosity model. The WLR model has been reported to provide better predictions than many other models (Werner et al., 2004). *Program*: HYDRUS2/3D.

6. *Modification*: Include the ability to model mid-simulation post-application "tarp-cutting" (removal). *Purpose:* This modification provides additional capability to simulate flux under actual use practices. *Programs*: HYDRUS1-D and HYDRUS2/3D.

7. *Modification*: provide the ability to simulate two different volatilization boundary conditions at the soil surface (e.g. tarped and untarped). *Purpose*: This modification will allow simulation of tarped bed fumigant applications where only a portion of the field is tarped. *Program*: HYDRUS2/3D.

Additional modifications may be implemented in the future. The purpose of this report is document the computational testing of the modifications listed above.

II. OVERVIEW

The modifications to the HYDRUS1D and HYDRUS2/3D models were tested in two phases. The objective of Phase 1 testing was to verify that when the modified models were run without any of the new features, they gave the same results as the existing unmodified models. Deviations between the unmodified and modified models in those scenarios would indicate that inadvertent errors were introduced during modification of the program codes. The most current unmodified model versions used in Phase 1 testing were HYDRUS1D ver. 4.14 and HYDRUS2/3D ver. 1.10 (Standard 2D version).

Phase 2 model testing was conducted to evaluate the actual modifications to the program code. A variety of approaches were used in Phase 2 depending on the particular modification. These are explained below under Phase 2 testing.

Note that in the following discussion, lower case "t" indicates units of time, while upper case "T" indicates units of temperature.

III. PHASE 1 TESTS

A. HYDRUS1D

Two of the HYDRUS authors, Drs. Jirka Šimůnek and Rien van Genuchten, presented a HYDRUS course to DPR in Sacramento in June 2008. In that course they provided several example HYDRUS1D fumigant modeling projects to demonstrate model features. These projects were fumig1, fumig1a, fumig2, fumig3, fumig4, and fumig4a. The projects served as the basis of Phase 1 testing here to evaluate the computational integrity of the modified HYDRUS1D relative to the unmodified model. The projects are available for download from the HYDRUS web site at <http://www.pc-progress.com/Downloads/Tutorials/Fumigants_H1D.zip>, and are described in detail in <http://www.pc-progress.com/Downloads/Tutorials/Tutorial_H1D_301_Fumigants.pdf>. Each project is based on a fumigant broadcast application scenario with the fumigant initially evenly distributed between the 30–45 cm depth. The simulation time was 21 days in all cases. Other features of the fumig1–fumig4 scenarios are given in Table 1.

Table 1. Characteristics of HYDRUS1D projects used in Phase 1 testing

simulation scenario characteristics	**fung1**	**fumg1a**	**fumig2**	**fumig3**	**fumig4**	**fumig4a**
init. conc. specified as aqueous conc (M L_{wat}^{-3})	y	n	y	y	y	y
init. conc. specified as total conc (M L_{soil}^{-3})	n	y	n	n	n	n
heat transport and temperature dependence of Henry's law and degradation coefficients	n	n	n	n	y	y
presence of tarp	n	n	y	n	n	y
post-application water application	n	n	n	y	n	n

Variables compared:

The variables that were compared were the 21d (end-of-simulation) nodal water contents, temperature and fumigant aqueous concentration; 0–21 d flux time series, and 21d cumulative flux.

Output files used:

- BALANCE.OUT–cumulative flux and mass balance data
- NOD_INF.out–nodal water content, nodal fumigant water concentrations
- solute1.out –flux time series

Conclusion:

No discrepancies between the unmodified and modified model outputs were evident. For example, projects fumig1a, fumig3, and fumig4a include all of the characteristics in Table 1, and end of simulation nodal soil-water contents, soil temperature, fumigant liquid phase concentrations and cumulative flux were identical for the modified and unmodified model versions. The fumigant flux time series were also identical (e.g. Figure 1).

Figure 1. HYDRUS1D project fumig4a flux time series for modified and unmodified versions of HYDRUS1D.

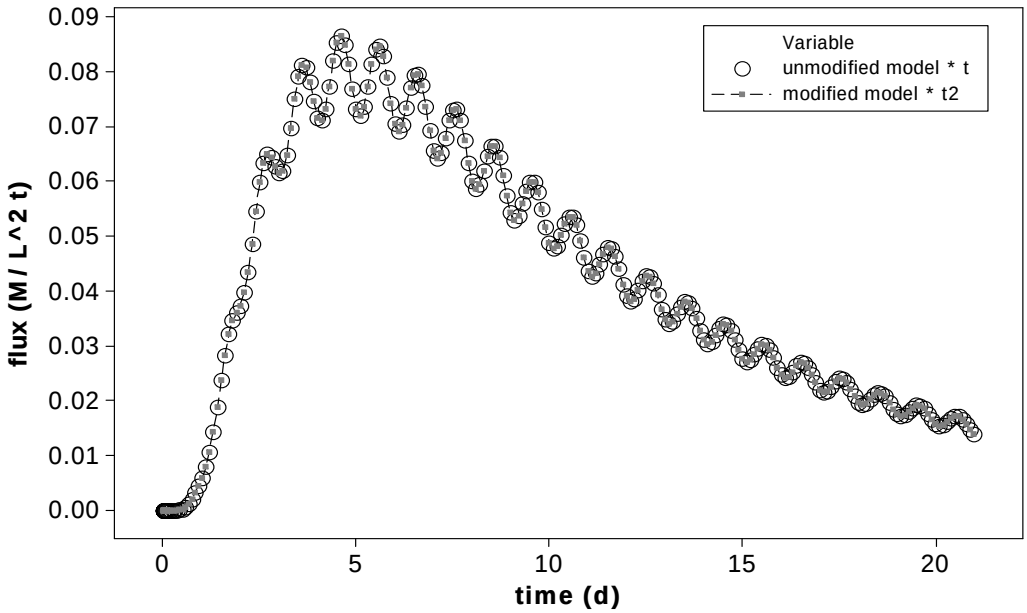

B. HYDRUS2/3D
Project used in testing:
The Phase 1 modeling scenario used for HYDRUS2/3D was a subsurface line source tarped fumigant application based on HYDRUS tutorial 3.05 (<http://www.pc-progress.com/en/Default.aspx?h3d-tutorials>). Water, solute and heat transport were simulated, and temperature dependence of the gas phase diffusion coefficient, Henry's law constant and 1st order degradation coefficients were also

considered. A pulse of fumigant was applied with water for 0.2 days from a 20 cm deep, 1 cm radius dripper to the 100 cm deep x 75 cm wide modeling domain. The upper surface of the transport domain was subject to a 500 cm boundary layer to simulate the presence of a tarp and the duration of the simulation was 7 d.

Variables compared:

7d (end-of-simulation) nodal water content, temperature and aqueous fumigant concentration; and 7d cumulative fumigant flux.

Output files used:

- conc1.txt, temp.txt, th.txt–exported text files of nodal aqueous fumigant concentration, temperature and water content, respectively
- solute1.out–fumigant flux time series, cumulative flux

Conclusion:

Program outputs compared well. Simulated fumigant flux from the two programs was nearly identical (Figure 2). Percent differences in nodal concentration, temperature and water content were calculated as:

[1] $$percent\ difference = \frac{unmodified\ output - modified\ output}{unmodified\ output}\ x\,100$$

Across all nodes in the transport domain, percent differences in aqueous fumigant concentration, temperature, and water content were in the range of–0.32% to 0.0006% (Table 2). The small differences in end of simulation nodal water content, temperature and fumigant aqueous phase concentration were attributable to small differences in numerical errors between the two programs. The cumulative flux of the modified model was 0.33% greater than the unmodified model, while end of simulation relative fumigant mass balance errors were 0.44%and 0.70% for the unmodified and modified simulations, respectively. No substantial differences between modified and unmodified model versions were evident.

Figure 2. HYDRUS2/3D phase 1 comparison of modified and unmodified models.

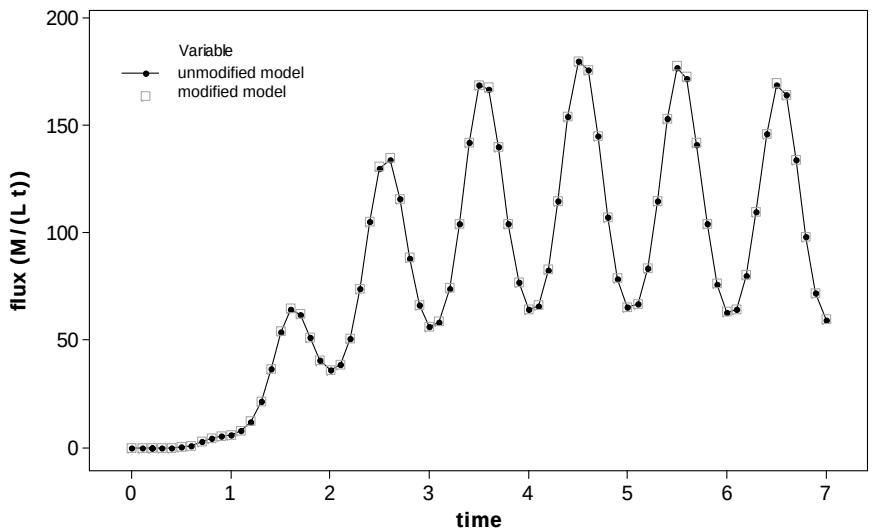

Table 2. End-of-simulation percent difference (Eq. 1) in nodal water contents, temperatures and fumigant aqueous concentrations between modified and unmodified HYDRUS2/3D models (N= 1079 nodes).

Nodal variable	minimum	median	maximum
water content	-1.2E-03	-5.6E-04	0
temperature	-6.8E-04	0	5.8E-04
concentration	-3.2E-01	-3.1E-01	-2.7E-01

IV. PHASE 2 TESTS

A. HYDRUS1D

1. New output file NOD_INF_C.out

A subsurface line source tarped fumigant application similar to that used in Phase 1 testing was run using both the modified and unmodified programs. Heat transport and temperature dependence were not simulated in this example so as to simplify gas phase concentration calculations. End of simulation nodal concentrations in NOD_INF_C.out were compared to calculations based on end of simulation nodal liquid concentrations in the unmodified HYDRUS1-D output file NOD_INF.out. Calculation formulae are given in appendix 1. The outputs were nearly identical, indicating the NOD_INF_C.out is calculating nodal concentrations correctly; the percent difference for each nodal concentration was in the range of -0.051% to 0.044% (Table 3).

Table 3. End-of-simulation percent difference (Eq. 1) between simulated and "hand-calculated" nodal concentrations for Phase 2 testing of new output file, NOD_INF_C.out (N=1079 nodes).

Variable	minimum	median	maximum
liquid concentration	-4.3E-02	-1.3E-03	3.5E-02
solid concentration	-4.1E-02	-1.3E-03	3.8E-02
gas concentration	-4.2E-02	-1.3E-03	3.9E-02
mass in liquid phase	-5.2E-02	-8.2E-03	4.1E-02
mass in solid phase	-4.4E-02	-1.9E-03	3.9E-02
mass in gas phase	-3.7E-02	3.2E-03	4.5E-02
total mass	-4.5E-02	-4.2E-03	3.6E-02

2. Temperature dependence of the stagnant surface boundary layer

In the HYDRUS programs, the flux J (M L^{-2} t^{-1}) at any given time is calculated as:

[2] $$J = \frac{D_g}{d(T)} C_g$$

where D_g is the gas phase diffusion coefficient (L^2 t^{-1}) and d(T) is a function giving the temperature dependent boundary layer thickness (L). Eq. [2] assumes that the concentration distant from the soil surface (i.e. at the top of the boundary layer) is zero. The function d(T) is given by:

[3] $$d(T) = d_{ref} \exp[\frac{E_a}{R}(\frac{1}{T_{ref}} - \frac{1}{T})]$$

where d_{ref} is the boundary layer thickness at the reference temperature T_{ref} = 293.15K, E_a is the activation energy (joules mol^{-1}), R is the gas constant (= 8.314 joules mol^{-1}) and T is the temperature (K).

Finally, when the HYDRUS sine wave soil surface temperature model is used, the temperature T at any time t is given by:

[4] $$T(t) = 273.15 + T_0 + A\, sin(\frac{2\pi t}{p} - \frac{7\pi}{12})$$

where T_0 is the mean soil surface temperature (degrees centigrade), p is the period (typically =1 day) and A is the amplitude of the sine wave in degrees.

The performance of the temperature dependent boundary layer option was evaluated by simulating volatilization from a soil column at an initial uniform fumigant concentration, and invoking the sine wave temperature model at the soil surface. Eqs. 2 - 4 were used in conjunction with the HYDRUS1D predicted gas phase concentration at the soil surface (C_g, eq. 2) to calculate flux at specific time steps. The calculated fluxes agreed well with the HYDRUS simulated fluxes (Fig. 3). Although small, percent difference between modeled and "hand

calculated" results are not shown. The modeled results are an average based on two values due to the Crank-Nicholson numeric solution scheme (J. Šimůnek, personal communication). Thus, at least a portion of any deviation between modeled and "hand" calculated results are due to averaging.

Figure 3. Test of temperature dependent boundary layer option. Calculated vs. simulated flux for HYDRUS 1-D. Diurnal variation in flux due to boundary layer temperature dependence.

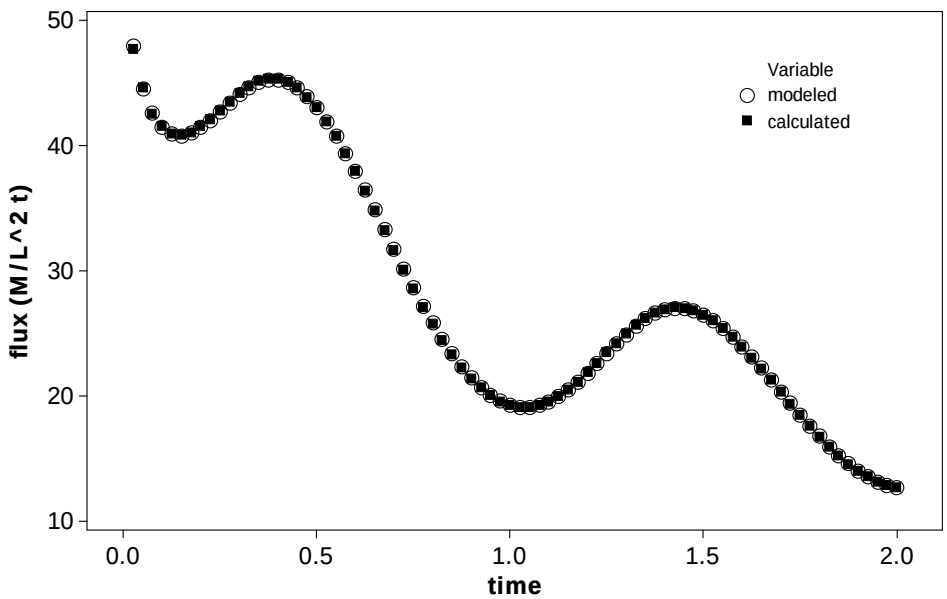

3. Mid-simulation tarp removal at specified time

The tarp removal option was tested using the fumig4A project by directly comparing end of simulation nodal water content, temperature and aqueous fumigant concentrations, and cumulative flux time series obtained from the unmodified program and the modified program. For the modified program, tarp removal was specified at 7d. The total simulation time was 21d.

For the unmodified program (no tarp removal option), a 7d tarped application was first simulated. End of simulation nodal water content, temperature and fumigant concentration were then used as initial conditions for a second 14d untarped simulation. The cumulative flux time series were nearly identical (Figure 4), with percent difference in total 21d cumulative fluxes of 0.7%. End of simulation nodal water contents, temperatures and aqueous phase fumigant concentrations of the two model versions compared favorably (Table 4).

Figure 4. Cumulative flux time series for modified and unmodified HYDRUS1D simulations of project fumig4a with tarp cutting simulated at day 7.

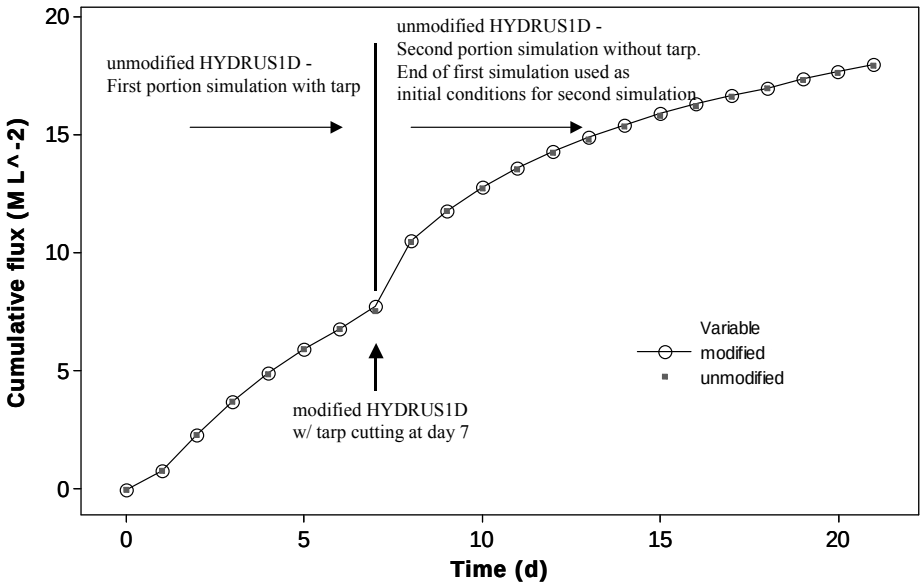

Table 4. End-of-simulation percent difference (Eq. 1) in nodal water contents, temperatures and fumigant aqueous concentrations for Phase 2 testing of tarp-cutting option using project fumig4a (N= 150 nodes).

Nodal variable	minimum	median	maximum
water content	0	0	0
temperature	0	5.0E-02	1.0E-01
concentration	-6.1E-02	0.0E+00	7.9E-02

4. Mid-simulation applications at a specified time and location in profile

The mid-simulation application option was tested using the fumig1a project (Table 1) as a basis for further modifications. A similar testing procedure to the mid-simulation tarp removal was employed: three separate projects were created, a 7d, 14d, and 21d simulation. The unmodified 7d simulation's final nodal water contents were used as initial conditions for the unmodified 14d project. The modified 21d simulation was conducted with a mid-simulation application specified at 7 days, equal to the mass applied at the start of the 14d simulation. The final nodal solute concentrations of the 14d simulation (unmodified) and 21d simulation (modified) were compared. The resulting final nodal total concentrations were essentially identical (Figure 5), with percent differences around -0.15 for all concentrations (Table 5).

Figure 5. Final total concentrations for modified and unmodified HYDRUS1D simulations of project fumig1a with a mid-simulation application.

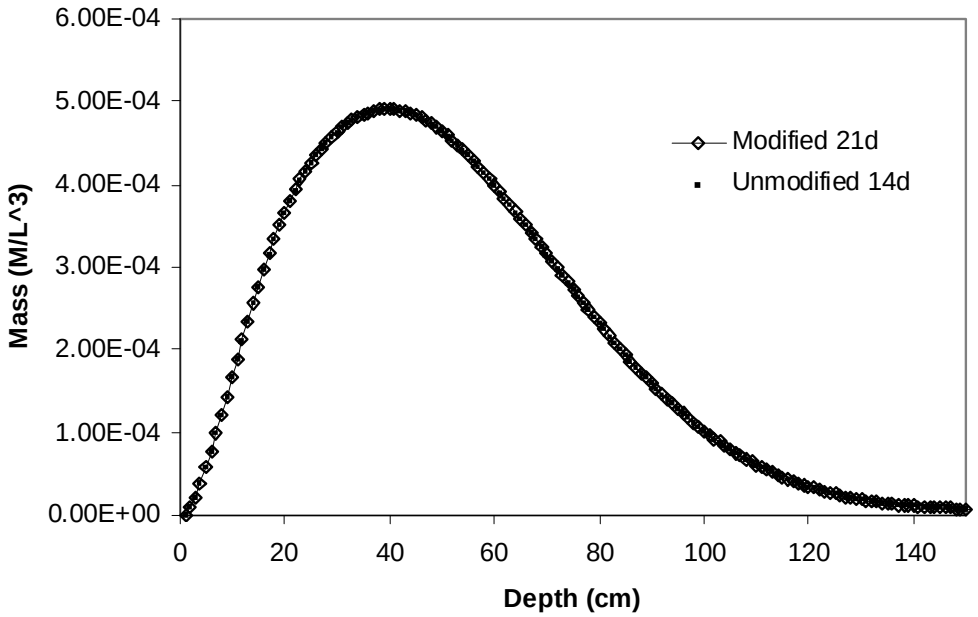

Table 5. End-of-simulation percent difference (Eq. 1) in nodal concentrations utilizing the mid-simulation application modification in HYDRUS1D (N = 150 nodes).

Variable	minimum	median	maximum
liquid concentration	-2.6E-01	-1.4E-01	-1.0E-01
solid concentration	-2.6E-01	-1.4E-01	-1.1E-01
gas concentration	-2.6E-01	-1.4E-01	-1.0E-01
mass in liquid phase	-3.0E-01	-1.5E-01	-1.0E-01
mass in solid phase	-2.6E-01	-1.4E-01	-1.1E-01
mass in gas phase	-2.5E-01	-1.4E-01	-9.8E-02
total mass	-2.7E-01	-1.5E-01	-1.1E-01

B. HYDRUS2\3D

1. New output file NOD_INF_C.out

The procedure for comparing the new nodal concentrations in the modified HYDRUS2/3D program to the unmodified program was the same as in the HYDRUS1D testing of NOD_INF_C.out. The modeling scenario was the subsurface line source tarped fumigant application used for the HYDRUS2/3D Phase 1 testing. Final nodal concentrations from the modified program's NOD_INF_C.out file were compared to final nodal concentrations, "hand

calculated" from liquid concentrations, in the unmodified HYDRUS2/3D output. The two sets of results were similar, with differences at a fraction of a percent (Table 6).

Table 6. End-of-simulation percent difference (Eq. 1) in nodal concentrations for Phase 2 testing of new output file, NOD_INF_C.out, in HYDRUS2D/3D (N=1079 nodes).

Variable	minimum	median	maximum
liquid concentration	-4.9E-03	0.0E+00	4.9E-03
solid concentration	-4.7E-03	8.5E-05	4.6E-03
gas concentration	-4.9E-03	0.0E+00	4.9E-03
mass in liquid phase	-3.3E-02	1.4E-02	3.5E-02
mass in solid phase	-4.5E-03	9.9E-05	4.8E-03
mass in gas phase	-2.3E-02	-1.1E-02	2.5E-02
total mass	-1.5E-02	7.1E-03	1.9E-02

2. Specification of initial nodal concentrations on total concentration basis
The same subsurface line source modeling scenario was used to compare specification of initial concentrations in terms of "liquid" concentration to "total" concentration, where total concentration = liquid phase + solid phase + gas phase solute, expressed as mass solute/volume bulk soil. The two initial condition specification methods yielded identical total- and phase specific solute concentrations.

3. Temperature dependence of the stagnant surface boundary layer
The testing method for the HYDRUS2/3D temperature dependent boundary layer option was identical to that used for HYDRUS1-D (section IV.A.2., above). In short, flux from a rectangular transport domain with constant initial uniform fumigant soil concentration was calculated at different times from simulated soil surface nodal concentrations from HYDRUS2/3D, the soil surface temperature as a (sine) function of time, calculated boundary layer thickness as a function of time and the specified diffusion coefficient (Eqs. 2–4). Similar to results for the temperature dependent boundary condition test in HYDRUS1-D, it's evident that flux based on modeled and "hand" calculated boundary layer thicknesses are essentially identical (Figure 6).

Figure 6. Test of temperature dependent boundary layer option. Calculated vs. simulated flux for HYDRUS2/3D. Diurnal variation in flux due to boundary layer temperature dependence.

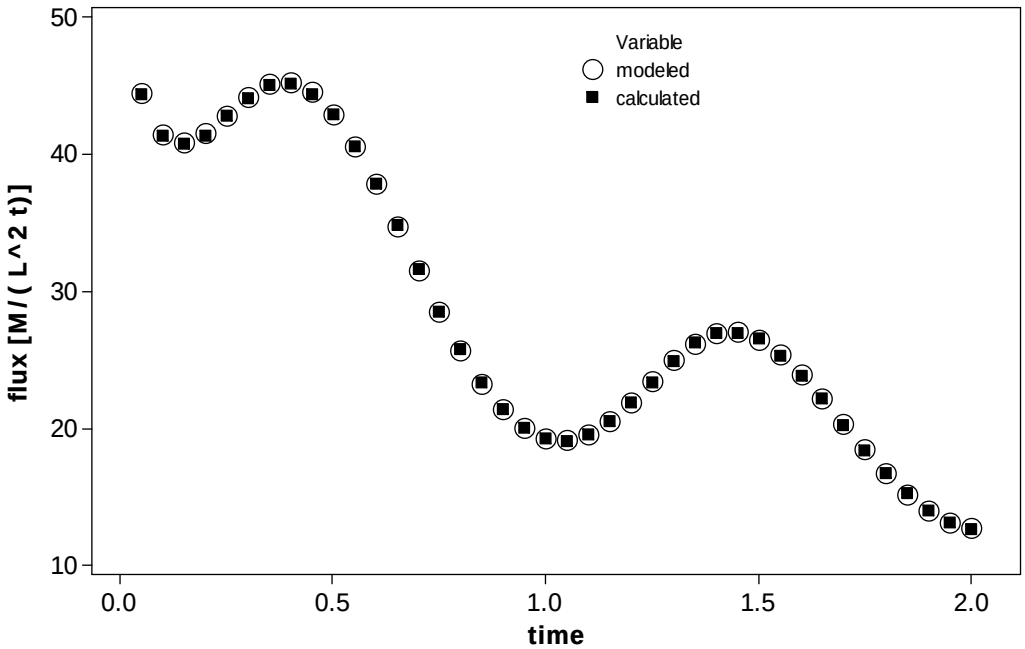

4. Mid-simulation tarp removal at specified time

The Phase 2 test of the HYDRUS2/3D tarp cutting option followed the same procedure as in the HYDRUS1D test of that same option: The unmodified program was run for seven days with a tarp, and the resultant nodal water content, temperature and fumigant concentrations were used as initial conditions for a second 14d simulation without tarping. The modeling scenario consisted of a rectangular transport domain with a constant initial fumigant concentration in soil at the 25–45 cm depth. The presence of a tarp was simulated using a stagnant surface boundary layer d = 500 cm. At the time of tarp removal, the modified HYDRUS2/3D program changes d back to a value appropriate for a bare soil surface (i.e. d = 0.5 cm).

The cumulative flux time series were nearly identical (Figure 7), with percent difference in total 21d cumulative fluxes of 0.7%. End of simulation nodal water contents, temperatures and aqueous phase fumigant concentrations of the two model versions compared favorably (Table 7).

Figure 7. Cumulative flux time series for modified and unmodified HYDRUS2/3D simulations of project fumig4a with tarp cutting simulated at day 7.

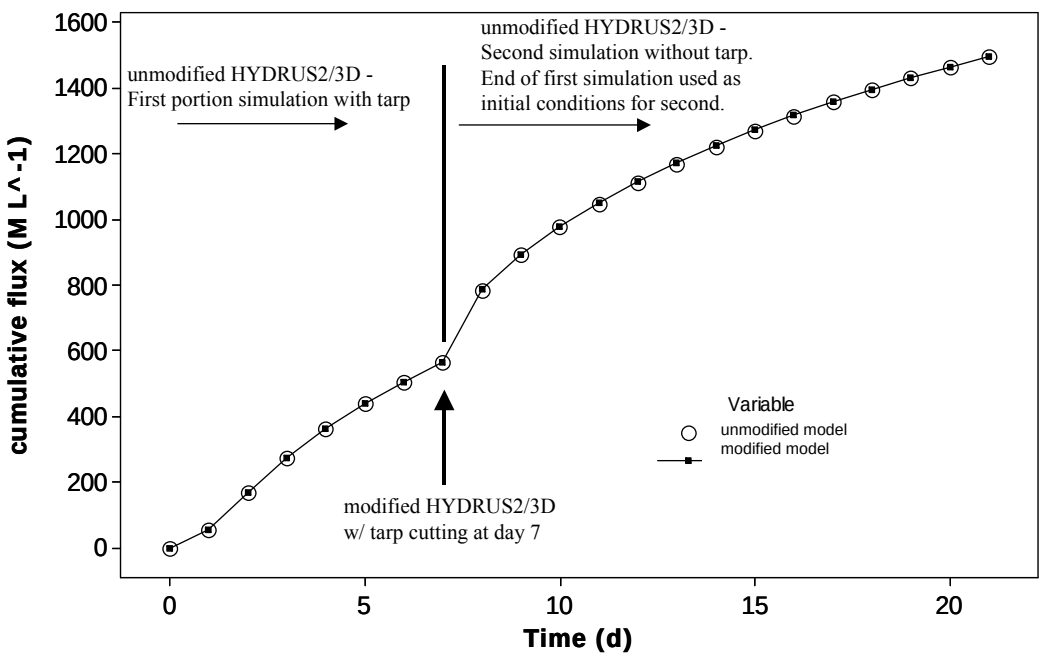

Table 7. End-of-simulation percent difference (Eq. 1) in nodal water contents, temperatures and fumigant aqueous concentrations for Phase 1 testing using project fumig3a (N= 1079 nodes).

Nodal variable	minimum	median	maximum
water content	-8.5E-06	0	8.6E-06
temperature	-1.0E-05	0	9.2E-06
concentration	-9.3E-06	0	1.2E-05

5. Alternative formulation of gas phase tortuosity

Diffusive transport of a gas in soil depends on the volume fraction of air-filled pores, the geometry of those pores and their "interconnectedness." The latter two characteristics are described in vadose transport models by the gas phase tortuosity τ_g ($0 < \tau_g < 1$). The net effect of τ_g in models such as HYDRUS is to directly scale (reduce) the effective gas phase diffusion coefficient by a factor of τ_g. Consequently, the effective diffusion coefficient D_{eff} ($=\tau_g * D_g$) is actually used in internal model calculations when tortuosity is considered. While most models use a Millington–Quirk (1961) type model to calculate τ_g from air-filled porosity a_v and saturated

water content θ_s (e.g. Šimůnek, 2006), Moldrup and co-workers introduced a "Water Linear Reduction Model" (WLR) as an alternative (Moldrup et al., 2006).

[5] $$\tau_g = \frac{a_v^{1.5}}{\theta_s}$$

Implementation of the WLR model was tested in HYDRUS2/3D using two simulations of diffusive transport only for an initial "plug" of solute in the center of a long horizontal column (Figure 8). The WLR model was used in the first simulation with $\theta_s = 0.400$, $a_v = 0.26898$ and $D_g = 300$. This yielded a WLR tortuosity factor of 0.34876 and $D_{eff} = 104.626$. The second simulation did not include either tortuosity model, and that simulation used a "scaled" gas phase diffusion coefficient $D_g = D_{eff,\ 1st\ simulation} = 104.626$. The results were essentially identical (Figure 9), demonstrating correct implementation of the WLR tortuosity model.

Figure 8. Diffusion inside an infinite column with initial solute distribution: conc = C_0, $-w < x < w$; = 0 otherwise. Boundary conditions for all boundaries: water – zero flux, solute – zero flux.

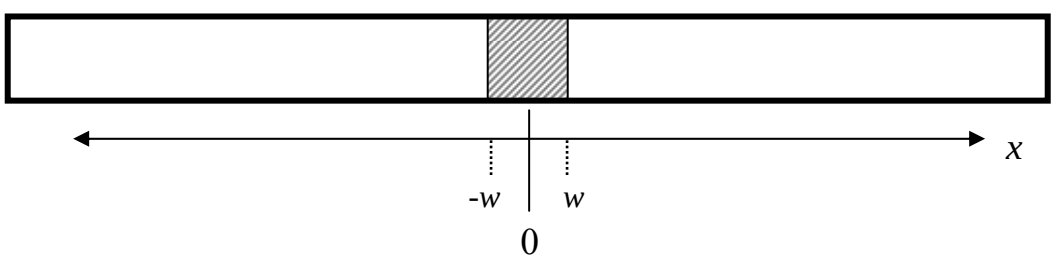

Figure 9. End-of-simulation liquid solute distributions for the Moldrup WLR tortuosity model and a simulation without tortuosity but identical D_{eff} as the first case.

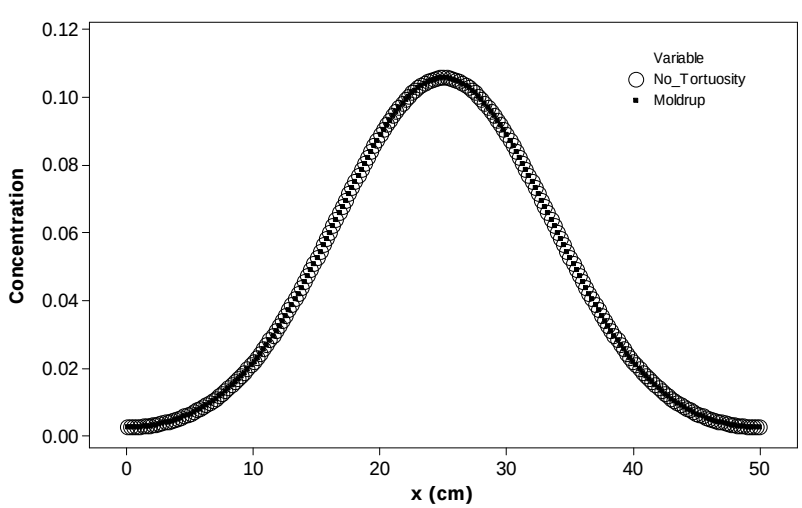

6. Mid-simulation applications at a specified time and location in profile
A similar procedure to the HYDRUS1D testing of mid-simulation applications was used in testing the HYDRUS2D/3D version of the same option. The end of simulation nodal water contents of an unmodified 7day run were used as the initial conditions of an unmodified 14d run. The output of a modified 21d simulation, with a mid-simulation application at 7 days equal to the mass applied at the start of the 14d simulation, was compared to the output of an unmodified 14d simulation (Figure 10). Nodal concentrations of both simulations were analogous to one another, with percent differences several orders of magnitude below one (Table 8).

Figure 10. Final total concentrations for modified and unmodified HYDRUS2D/3D simulations with a mid-simulation application. Note that node numbers in HYDRUS2/3D are assigned during the mesh generation step and do not necessarily display any obvious geometric configuration, leading to unusual distributions of concentration as a function of node number. One hundred fifty of 232 total nodes shown above for clarity.

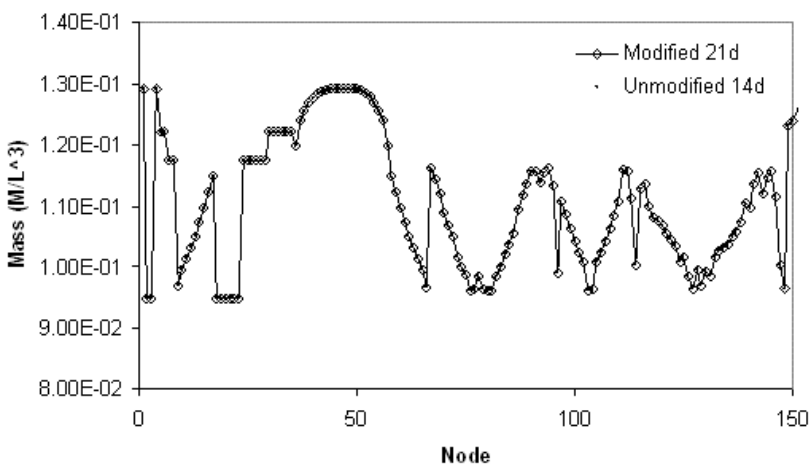

Table 8. End-of-simulation percent difference (Eq. 1) in nodal concentrations utilizing the mid-simulation application modification in HYDRUS2D/3D (N=232 nodes).

Variable	minimum	median	maximum
ConcL	-8.8E-03	-7.2E-03	0.0E+00
ConcS	-6.1E-03	-4.5E-03	-3.2E-03
ConcG	-6.1E-03	-4.5E-03	-3.2E-03
MassL	-9.5E-03	-4.8E-03	0.0E+00
MassS	-1.0E-02	-4.7E-03	0.0E+00
MassG	-6.3E-03	-5.9E-03	0.0E+00
TotalMass	-1.0E-02	-6.5E-03	0.0E+00

7. Implementation of two different volatilization boundary conditions at soil surface
In HYDRUS2/3D, the volatile solute boundary condition (BC) simulates volatilization as a first-order mass transfer process through a stagnant boundary layer at the soil surface. The rate of diffusion is proportional to the concentration difference between the top and bottom of the boundary layer, and inversely proportional to the depth of a stagnant boundary layer *d*. The boundary layer depth is adjustable and provides mass transfer resistance at the surface. To simulate the presence of a tarp, an equivalent *d* is chosen to represent the mass transfer resistance of the tarp (Spurlock, 2010). To simulate volatilization from a bare soil surface, *d* = 0.5 cm is typically assumed (Jury et al. 1983, Simunek et al., 2006).

The unmodified HYDRUS2/3D version only allows specification of a single volatilization boundary condition, i.e. for all nodes where volatilization is simulated, a single mass transfer resistance must be used. This shortcoming prevents realistic simulation of certain scenarios such as tarped bed applications (Figure 11).

Figure 11. Example of bedded tarp fumigant application where shallow fumigant shank applications are immediately followed by the bed shaping/tarping process.

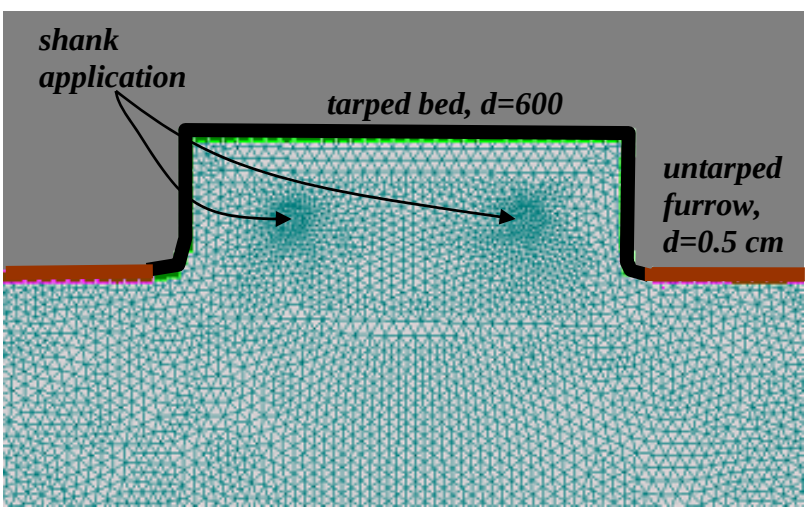

HYDRUS2/3D was modified to remedy this shortcoming. The modified version now allows two different volatile solute BCs to be specified at the soil surface. The first volatilization condition is as before, where a stagnant boundary layer of user-defined depth is specified. This volatilization BC is specified for nodes where the water flow BC is "Atmospheric." The second volatilization BC is a "bare-soil" volatilization BC where the stagnant boundary layer thickness is constant = 0.5cm. The second BC may be specified only for nodes in which the water flow BC is "variable flux 1."

The performance of this BC was investigated using a modeling scenario consisting of a rectangular transport domain with a constant initial fumigant concentration at the 20-40cm depth. There were 19 nodes across the upper boundary. Unlike the previous modeling comparisons, it was not possible to devise a simulation with the unmodified version of Hydrus2/3D which would mimic the computations of the modified Hydrus2/3D for the implementation of two different volatilization boundary conditions at soil surface. Therefore, instead of a modified to unmodified comparison, a series of simulations was conducted to check for the consistency of distributed versus clumped untarped areas versus tarped surface fraction. Thirteen simulations were performed using different nodal combinations of the two volatilization BCs (Figure 12).

Simulations 1 and 8 (Figure 12) both simulated bare ground emissions using $d = 0.5$ cm at all nodes. In 1, the water flow boundary condition was atmospheric, so this simulation corresponded to the volatilization BC as it has previously been implemented. In simulation 8, the water flow boundary condition was "variable flux 1," so that simulation utilized only the modification. The total flux in the two cases were essentially equal (Figure 12), demonstrating the equivalence of the "bare ground" volatilization BC for the two cases.

Figure 12. Investigation of modified HYDRUS2/3D volatilization boundary condition. For untarped nodes, boundary layer depth = 0.5 cm; for tarped nodes, boundary layer depth d = 600 cm. Flux ratio = (mass fumigant volatilized at end of simulation/total initial application).
In the remaining simulations, the effect on flux of numbers of untarped nodes, and configuration of those nodes were investigated. The configuration "centered" refers to simulations 3 and 8 – 13, where the untarped nodes are adjacent and centered on the surface. The configuration "distributed" refers to simulations 3 – 8 where the untarped nodes are evenly spaced across the surface. It's apparent that even when a small fraction of the surface is untarped, large increases in flux relative to the tarped case may be observed (*cf.* simulations 2 – 4).

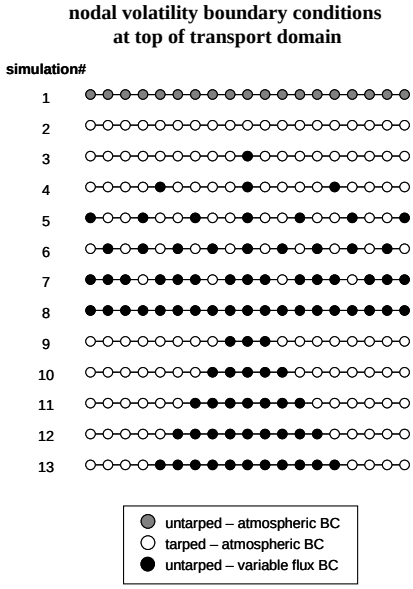

no. untarped nodes	fraction surface untarped	tarped area flux	untarped area flux	total flux ratio
19	1.000	---	2795	0.499
0	0.000	1081	---	0.193
1	0.056	822	723	0.276
3	0.167	451	1710	0.386
7	0.389	204	2324	0.451
9	0.500	96.6	2576	0.477
15	0.778	37.5	2719	0.492
19	1.000	----	2809	0.501
3	0.167	655	1171	0.326
5	0.278	524	1512	0.363
7	0.389	405	1818	0.396
9	0.611	296	2091	0.426
11	0.778	193	2336	0.451

In addition, the distribution, as well as amount, of untarped area influences flux ratio (Figure 13). The higher fluxes observed for the distributed configurations are attributable to shorter mean diffusion pathways for fumigant molecules at the surface. Figure 14 shows how the modified boundary condition affects fumigant soil concentration across the surface using simulation 4. Finally, Figure 15 is an illustrative example of the dual volatilization boundary condition for a bedded tarp application, where the bed portion of the field is covered by a tarp and the furrows are untarped. The diurnal fluctuations in cumulative flux result from temperature dependence of D_g, Henry's constant and tarp permeability.

Figure 13. Flux ratios vs fraction surface area untarped for distributed and centered untarped nodal configurations (Figure 12).

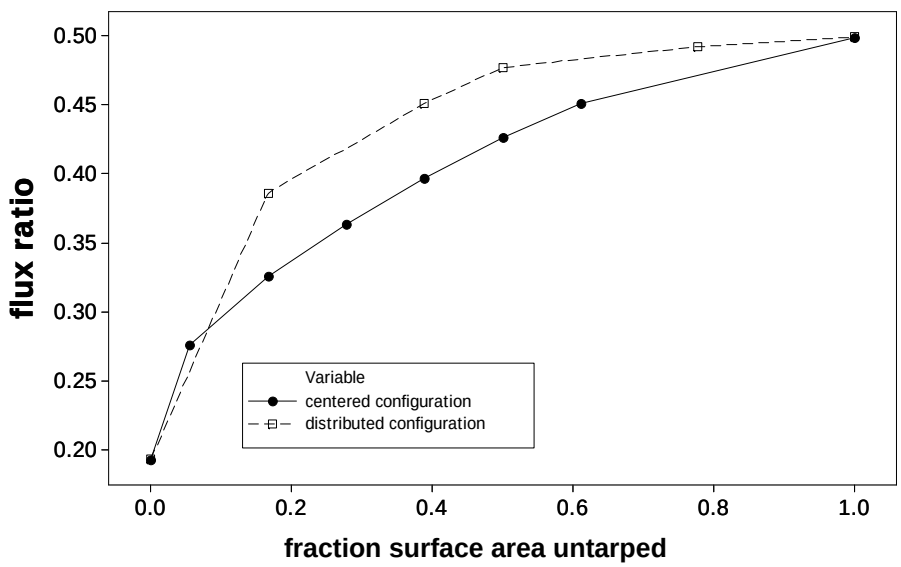

Figure 14. End of simulation fumigant distribution for 3 distributed untarped nodes (case 4, Figure 12).

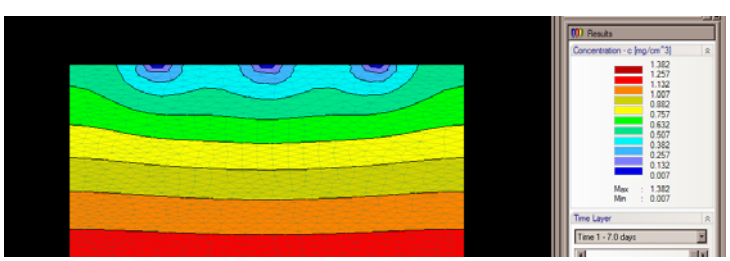

Figure 15. Illustrative example of dual volatilization boundary condition simulation for bedded tarp application. Immediately after fumigant injection, bed is shaped and tarped. In cumulative flux plots, the "atmospheric solute flux" is the cumulative flux through the tarped region (delineated by the white line), while the "variable boundary flux 1" is the cumulative flux through the (untarped) furrow. *Note color concentration scale is different for each picture.*

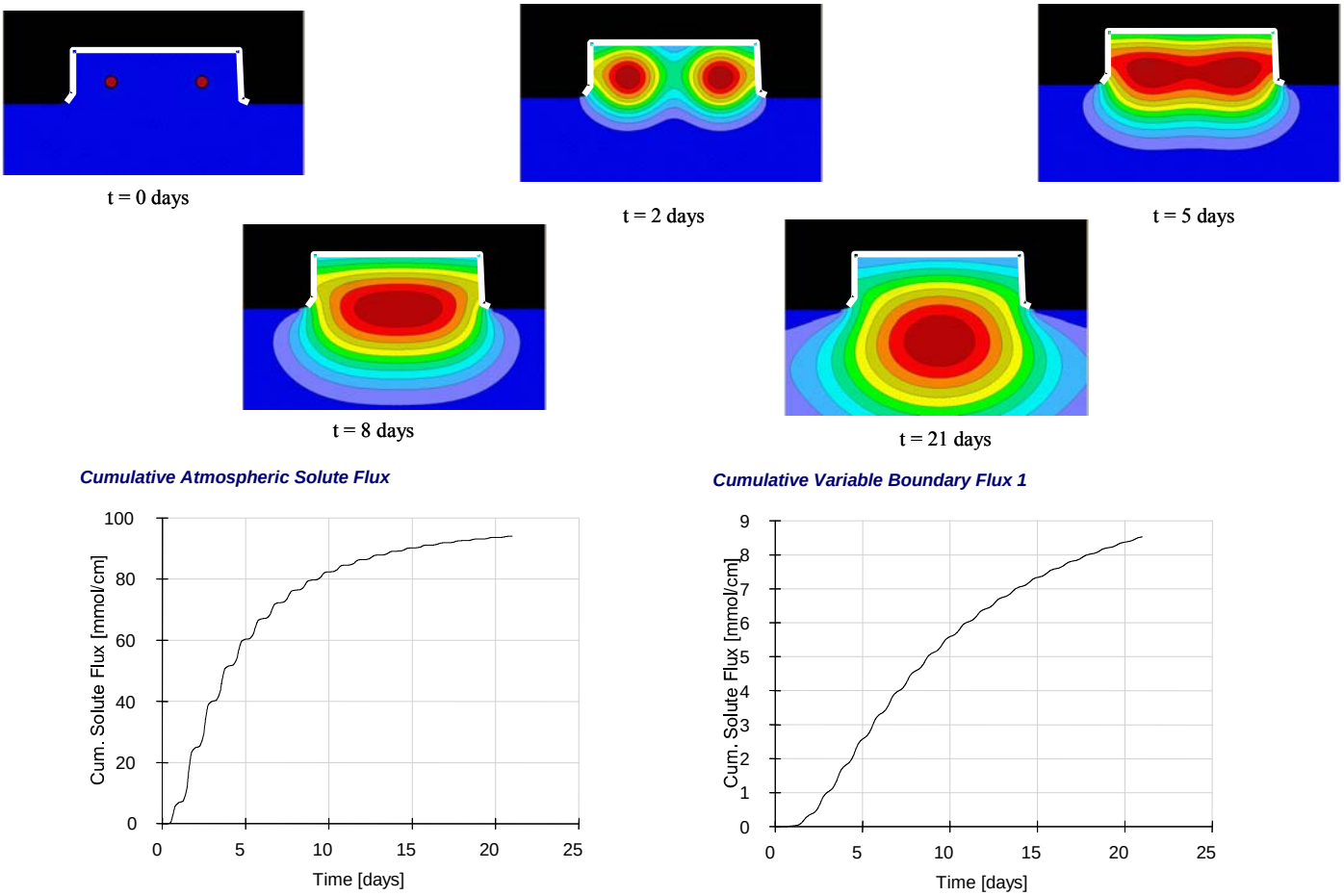

V. CONCLUSION

Based on the testing conducted, the modified HYDRUS1-D and HYDRUS2/3D programs perform as expected. No errors were evident in the modified programs.

VI. REFERENCES

Jury, W. A., W. F. Spencer, and W. J. Farmer, Behavior assessment model for trace organics in soil, I. Model description, J. Environ. Qual., 12, 558-564, 1983.

Millington, R.J. and J.P. Quirk. 1960. Transport in porous media. p. 97-106. In F.A. Van Beren et. Al (eds). Trans. 7th International Congress of Soil Science, Vol. 1, Madison, WI, Aug. 14-24. Amsterdam, The Netherlands.

Millington, R.J. and J.P. Quirk. 1961. Permeability of porous solids. Transac. Faraday Soc. 57:1200-1207.

Moldrup, P., T. Olesen, J. Gamst, P. Schjonning, T. Yamaguchi, and D.E. Rolston. 2000. Prediciting the gas diffusion coefficient in repacked soil: Water-induced linear reduction model. Soil Sci. Soc. Am. J. 64: 1588-1594.

Papiernik, S. and S.R. Yates. 2002. Effect of Environmental Conditions on the Permeability of High Density Polyethylene Film To Fumigant Vapors. Environ. Sci. Technol. 36:1833-1838.

Šimůnek, J., M. Šejna, H. Saito, M. Sakai, and M. Th. van Genuchten. 2009. The HYDRUS-1D Software Package for Simulating the One-Dimensional Movement of Water, Heat, and Multiple Solutes in Variably-Saturated Media. User Manual version 4.08. Available at: <http://www.pc-progress.com/en/Default.aspx?programs>.

Šimůnek, J., M. Th. van Genuchten and M. Šejna. 2006. The HYDRUS Software Package for Simulating the Two- and Three-Dimensional Movement of Water, Heat, and Multiple Solutes in Variably-Saturated Media. Technical Manual. version 1. Available at: <http://www.pc-progress.com/en/Default.aspx?programs>.

Spurlock, F. 2008. Fumigant Transport Modeling Using HYDRUS: Estimation of Soil Hydraulic Parameters Using Pedotransfer Functions. August 14, 2008 memorandum to: R. Segawa. Available at: <http://www.cdpr.ca.gov/docs/emon/pubs/ehapreps/analysis_memos/2066_rosetta.pdf>.

Spurlock, F. 2009. Fumigant Transport Modeling Using Hydrus: 2. Comparison of Model Simulations to Analytical Solutions of Fick's Second Law of Diffusion. Available at: <http://www.cdpr.ca.gov/docs/emon/pubs/ehapreps/analysis_memos/2163_segawa.pdf>.

Spurlock, F. 2010. Fumigant Transport Modeling Using Hydrus: 3. Fumigant Transport Modeling Using Hydrus: 3. Selection, Temperature Dependence and Sensitivity Analysis of Fumigant Physicochemical Properties. Available at: <http://www.cdpr.ca.gov/docs/emon/pubs/ehapreps/analysis_memos/2077_segawa.pdf>.

Werner, D., P. Grathwohl, and P. Höhener, Review of field methods for the determination of the tortuosity and effective gas-phase diffusivity in the vadose zone, *Vadose Zone J.*, *3*, 1240-1248, 2004.

APPENDIX 1
DOCUMENTATION FOR MODIFIED FEATURES

HYDRUS-1D and HYDRUS (2D/3D) Modifications to Simulate and Analyze the Transport of Fumigants

Jiří Šimůnek

Department of Environmental Sciences
University of California Riverside
Riverside, CA 92521

Agreement No 09-C0078
Department of Pesticide Regulation
Environmental Monitoring Brach
1001 I Street 4th Floor
Sacramento, CA 95814

Appendix Contents:

1. **New Output File Nod_inf_c.out**
2. **Total Initial Nodal Concentrations**
3. **Temperature Dependence of the Stagnant Surface Boundary Layer**
4. **Tarp Removal at a Specified Time**
5. **Alternative Formulations for the Gas Phase Tortuosity**
6. **Application of a Fumigant at a Specified Time and Location**
7. **Two Different Volatilization Boundary Conditions at the Soil Surface**
8. **References**
9. **HYDRUS-1D and HYDRUS (2D/3D) Test Examples**
10. **The Fumigants.in Input File**

1. New Output File Nod_inf_c.out

A new output file (Nod_inf_c.out) is created by both HYDRUS-1D and HYDRUS (2D/3D), which contains nodal coordinates, water contents, temperatures, and various forms of concentrations (i.e., liquid, solid, gaseous, and total). Below is an example of one time-level from this file. The file contains the following variables:

Node	Node Number
x,z	*x*- and *z*-coordinates
Wat	Water Content $[L_w^3 L_s^{-3}]$
ConcL	Liquid phase concentration $[M_c L_w^{-3}]$
ConcS	Solid phase concentration $[M_c M_s^{-1}]$
ConcG	Gas phase concentration $[M_c L_a^{-3}]$
MassL	Mass in the liquid phase, S_l $[M_c L_s^{-3}]$
MassS	Mass in the solid phase, S_s $[M_c L_s^{-3}]$
MassG	Mass in the gas phase, S_g $[M_c L_s^{-3}]$
TotalMass	Total Mass, $S=S_l+S_s+S_g$ $[M_c L_s^{-3}]$
Temper	Temperature [^{o}C]

Subscripts *w*, *c*, *a*, and *s* refer to water, contaminant, air, and soil.

Time: 21.0000

Node	z [L]	Wat	ConcL [M_c/L_w^3]	ConcS [M_c/M_s]	ConcG [M_c/L_a^3]	MassL [M_c/L_s^3]	MassS [M_c/L_s^3]	MassG [M_c/L_s^3]	TotalMass [M_c/L_s^3]	Temper [C]
1	.0000	.1041	.69356E-04	.12970E-04	.47329E-07	.72182E-05	.19454E-04	.16372E-07	.26689E-04	15.170
2	-1.0000	.1268	.11051E-02	.20666E-03	.14782E-05	.14016E-03	.30998E-03	.47772E-06	.45063E-03	15.730
3	-2.0000	.1407	.22697E-02	.42444E-03	.53651E-05	.31925E-03	.63666E-03	.16597E-05	.95756E-03	16.236
4	-3.0000	.1490	.35177E-02	.65781E-03	.13626E-04	.52399E-03	.98672E-03	.41021E-05	.15148E-02	16.702
5	-4.0000	.1547	.48150E-02	.90040E-03	.28762E-04	.74486E-03	.13506E-02	.84935E-05	.21039E-02	17.134
6	-5.0000	.1590	.61490E-02	.11499E-02	.53776E-04	.97751E-03	.17248E-02	.15650E-04	.27180E-02	17.532
7	-6.0000	.1625	.75174E-02	.14058E-02	.91971E-04	.12213E-02	.21086E-02	.26445E-04	.33564E-02	17.899
8	-7.0000	.1653	.89207E-02	.16682E-02	.14665E-03	.14745E-02	.25023E-02	.41753E-04	.40185E-02	18.235
9	-8.0000	.1674	.10357E-01	.19367E-02	.22072E-03	.17340E-02	.29050E-02	.62368E-04	.47014E-02	18.541
10	-9.0000	.1692	.11821E-01	.22106E-02	.31634E-03	.19996E-02	.33158E-02	.88843E-04	.54043E-02	18.817
. . . . .										
148	-147.0000	.1788	.48364E-02	.90440E-03	.31759E-03	.86482E-03	.13566E-02	.86125E-04	.23075E-02	19.993
149	-148.0000	.1788	.48096E-02	.89939E-03	.31583E-03	.86002E-03	.13491E-02	.85647E-04	.22948E-02	19.993
150	-149.0000	.1788	.47962E-02	.89688E-03	.31495E-03	.85763E-03	.13453E-02	.85409E-04	.22884E-02	19.993
151	-150.0000	.1788	.47962E-02	.89688E-03	.31495E-03	.85763E-03	.13453E-02	.85409E-04	.22884E-02	19.993

end

The table below describes how various variables are calculated.

	Equilibrium model	Mobile-immobile model	Two-site sorption model	Two-kinetic sites model
Liquid phase concentration $[M_c L_w^{-3}]$	c	$\frac{c_m\theta_m + c_{im}\theta_{im}}{\theta_m + \theta_{im}}$	c	c
Solute mass in the liquid phase, S_l $[M_c L_s^{-3}]$	$c\theta$	$c_m\theta_m + c_{im}\theta_{im}$	$c\theta$	$c\theta$
Gas phase concentration $[M_c L_a^{-3}]$	$K_H c$	$K_H c$	$K_H c$	na
Solute mass in the gas phase, S_g $[M_c L_s^{-3}]$	$K_H ca$	$K_H ca$	$K_H ca$	na
Solid phase concentration $[M_c M_s^{-1}]$	$K_D c$	$K_D\left[fc_m + (1-f)c_{im}\right]$	$f_e K_D c + s^k$	$s_1^k + s_2^k$
Solute mass in the solid phase, S_s $[M_c L_s^{-3}]$	$\rho K_D c$	$\rho K_D\left[fc_m + (1-f)c_{im}\right]$	$\rho\left(f_e K_D c + s^k\right)$	$\rho\left(s_1^k + s_2^k\right)$
Total solute mass, $S=S_l+S_s+S_g$ $[M_c L_s^{-3}]$				

a air content $[L_a^3 L_s^{-3}]$

c liquid phase concentration $[M_c L_w^{-3}]$

c_m liquid phase concentration in the mobile phase $[M_c L_w^{-3}]$

c_{im} liquid phase concentration in the immobile phase $[M_c L_w^{-3}]$

θ water content $[L_w^3 L_s^{-3}]$

θ_m water content in the mobile phase $[L_w^3 L_s^{-3}]$

θ_{im} water content in the immobile phase $[L_w^3 L_s^{-3}]$

K_D distribution (sorption) coefficient $[L_w^3 M_s^{-1}]$

K_H Henry's law constant [-]

S_l solute mass in the liquid phase $[M_c L_s^{-3}]$

S_s solute mass in the solid phase $[M_c L_s^{-3}]$

S_g mass in the gas phase $[M_c L_s^{-3}]$

S total solute mass, $S=S_l+S_s+S_g$ $[M_c L_s^{-3}]$

s solid phase concentration $[M_c M_s^{-1}]$

s^k solid phase concentration on kinetic sorption sites $[M_c M_s^{-1}]$

s_1^k solid phase concentration on first kinetic sorption sites $[M_c M_s^{-1}]$

s_2^k	solid phase concentration on second kinetic sorption sites $[M_c M_s^{-1}]$
f	fraction of sorption sites in contact with mobile water [-]
f_e	fraction of sorption sites with equilibrium sorption [-]
ρ	bulk density $[M_s L_s^{-3}]$

2. Total Initial Nodal Concentrations

Solute transport initial conditions can be specified either in terms of the liquid concentration c [ML^{-3}; mass of solute/volume of water] or in terms of the total concentration S [ML^{-3}; mass of solute/volume of soil]. The liquid phase concentration is in the latter case calculated for linear sorption as follows:

$$S = \theta c + \rho s + a_v\ g = \theta c + \rho K_D c + a_v K_H c = c(\theta + \rho K_D + a_v K_H)$$
$$c = \frac{S}{\theta + \rho K_D + a_v K_H} \tag{1}$$

and for nonlinear sorption by finding a root of the following nonlinear equation:

$$S = \theta c + \rho s + a_v\ g = \theta c + \frac{\rho K_D c^{\beta}}{1 + \eta c^{\beta}} + a_v K_H c \tag{2}$$

For the two kinetic sorption sites model (only a linear case is implemented, i.e., without blocking) the distribution coefficient k_s for is assumed to be defined as:

$$K_D = \frac{\theta k_a}{\rho k_d} \tag{3}$$

Rather than specifying directly concentrations in the nonequilibrium phases, the nonequilibrium phase concentration can be specified to be initially at equilibrium with equilibrium phase concentration. In such case, the immobile water content concentration will be set equal to the mobile water content concentration for the dual porosity models. The sorbed concentration at the kinetic sorption sites will be set equal to:

$$s = (1 - f) K_D c \tag{4}$$

for the linear sorption and:

$$s = (1 - f) \frac{\rho K_D c^{\beta}}{1 + \eta c^{\beta}} \tag{5}$$

for the nonlinear sorption. For the two kinetic sorption sites model, the sorbed concentrations are set equal to:

$$s = \frac{\theta k_a}{\rho k_d} c \tag{6}$$

where k_a and k_d are the attachment and detachment coefficients, respectively.

These options can be selected from the new section (Initial Conditions) of the Solute Transport - General Information dialog window (see below).

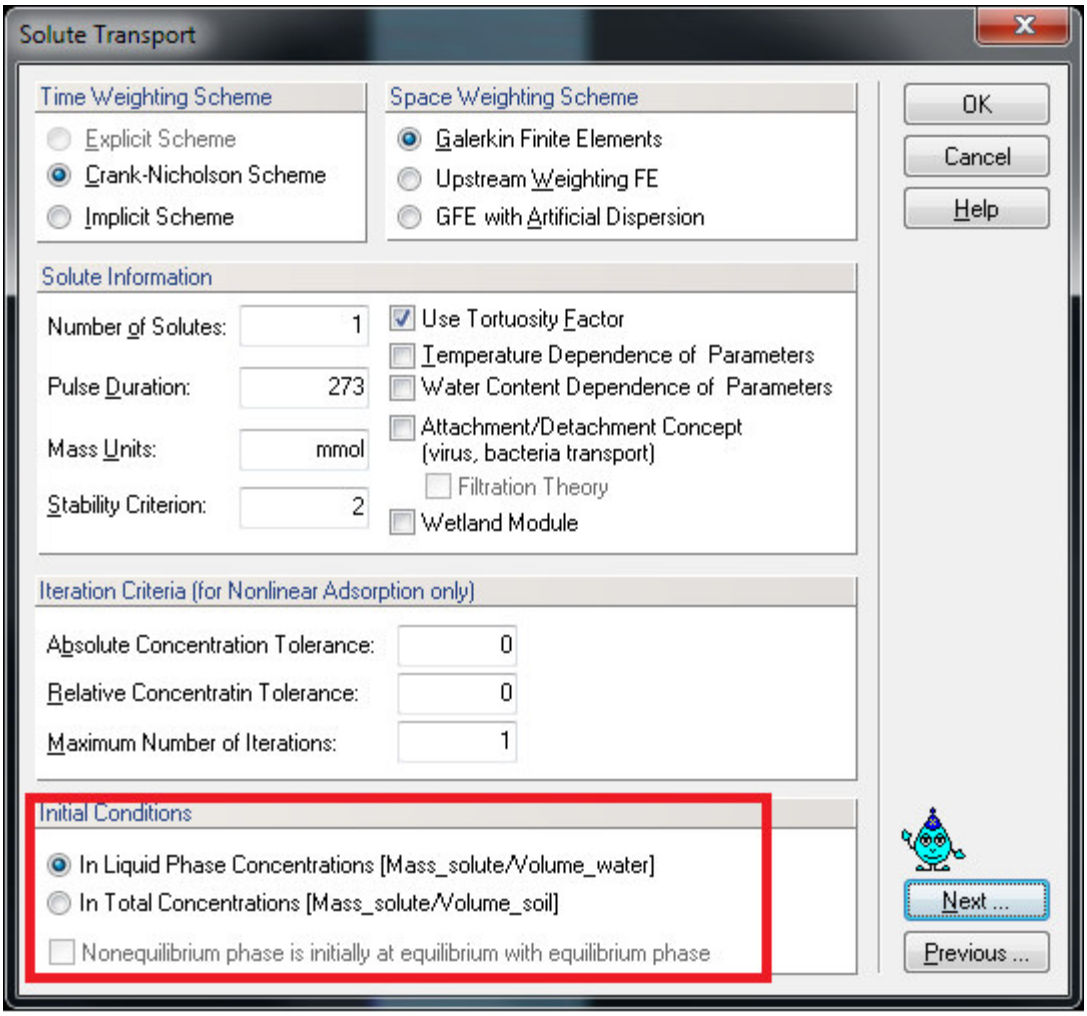
Solute Transport
Time Weighting Scheme
Explicit Scheme
Crank-Nicholson Scheme
Implicit Scheme
Space Weighting Scheme
Galerkin Finite Elements
Upstream Weighting FE
GFE with Artificial Dispersion
OK
Cancel
Help
Solute Information
Number of Solutes: 1
Pulse Duration: 273
Mass Units: mmol
Stability Criterion: 2
Use Tortuosity Factor
Temperature Dependence of Parameters
Water Content Dependence of Parameters
Attachment/Detachment Concept (virus, bacteria transport)
Filtration Theory
Wetland Module
Iteration Criteria (for Nonlinear Adsorption only)
Absolute Concentration Tolerance: 0
Relative Concentratin Tolerance: 0
Maximum Number of Iterations: 1
Initial Conditions
In Liquid Phase Concentrations [Mass_solute/Volume_water]
In Total Concentrations [Mass_solute/Volume_soil]
Nonequilibrium phase is initially at equilibrium with equilibrium phase
Next ...
Previous ...

3. Temperature Dependence of the Stagnant Surface Boundary Layer

Temperature dependence of the thickness of the stagnant surface boundary layer (i.e., a surface boundary layer through which volatile solutes dissolves to the atmosphere) was implemented in a similar way as for all other transport and reaction parameters using the Arrhenius equation [*Stumm and Morgan*, 1981]. After some modification, this equation can be expressed in the general

$$a_T = a_r \exp\left[\frac{E_a(T^A - T_r^A)}{R_u T^A T_r^A}\right] \tag{7}$$

where a_r and a_T are the values of the coefficient (the thickness of the stagnant surface boundary layer) being considered at a reference absolute temperature T_r^A and absolute temperature T^A, respectively; R_u is the universal gas constant, and E_a [$ML^2T^{-2}M^{-1}$] is the activation energy of the particular reaction or process being modeled.

In both HYDRUS-1D and HYDRUS (2D/3D), the activation energy of this factor is entered at the following location in the Temperature Dependent Solute Transport and Reaction parameters dialog window (see below).

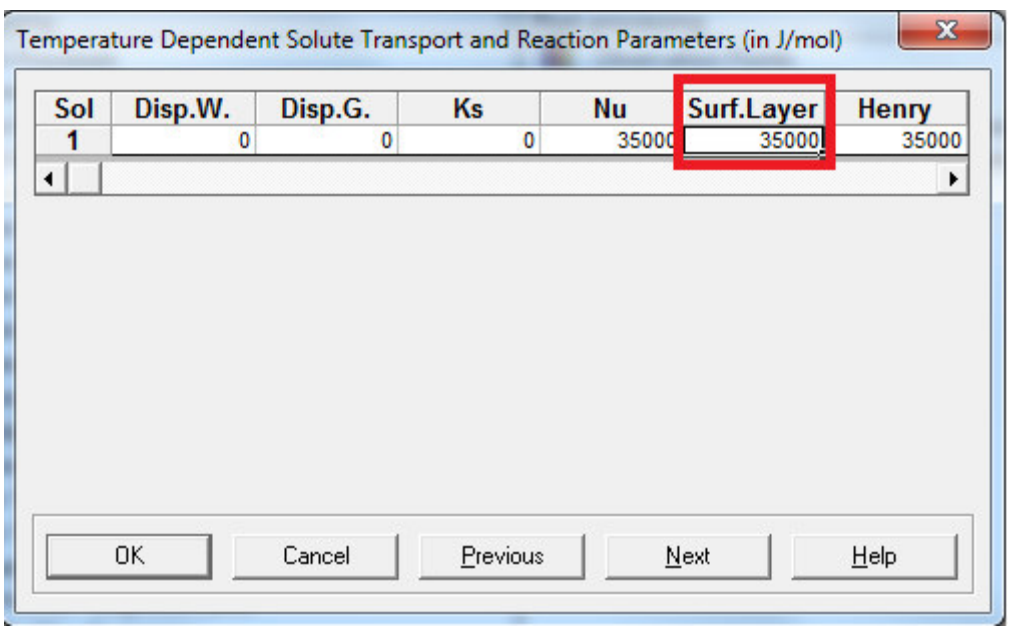

4. Tarp Removal at a Specified Time

In the modified computational modules simulating transport of fumigants, the Pulse Duration variable is used instead to represent the "Time of Tarp Removal". The variable is specified in the "Solute Transport - General Information" dialog window at the following locations in the HYDRUS-1D (left figure below) and HYDRUS (2D/3D) (right figure below)

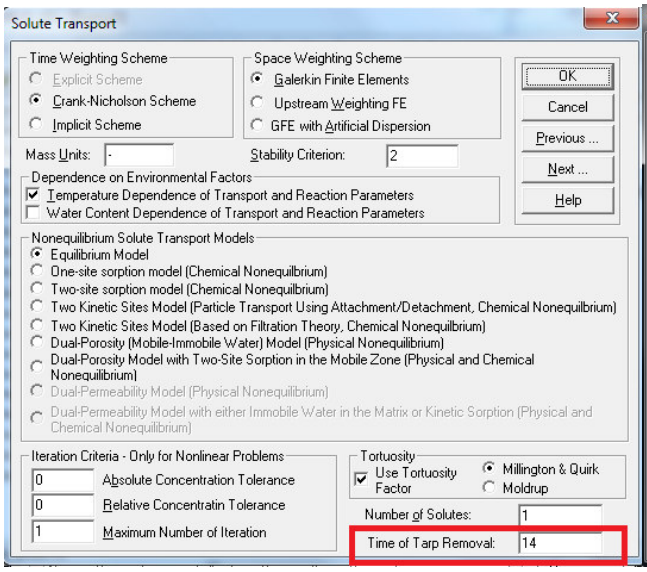

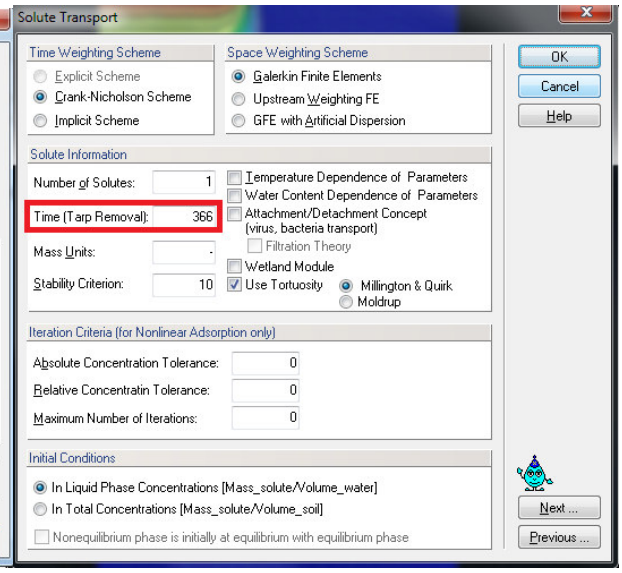

HYDRUS-1D **HYDRUS (2D/3D)**

After the tarp is removed, the stagnant boundary layer is assumed to have a constant thickness of $d = 0.5$ cm.

The Fumigant.in input file needs to be in the project folder and the lFumig variable has to be set to .true. for this option to be active.

5. Alternative Formulations for the Gas Phase Tortuosity

Alternative relationships are available in version 4.05 of HYDRUS-1D and higher to describe tortuosity coefficients in both phases. *Moldrup et al*. [2000] suggested the following formulation for calculating the tortuosity factor in the gaseous phase for sieved and repacked soils:

$$\tau_g = \frac{a_v^{1.5}}{\theta_s}$$

This formulation was found to provide superior predictions of several porosity-based relationships by *Werner et al.* [2004]. Similarly, *Moldrup et al*. [1997] suggested an alternative relationship for calculating the tortuosity coefficient in the liquid phase:

$$\tau_w = 0.66\left(\frac{\theta}{\theta_s}\right)^{8/3}$$

The *Millington-Quirk* [1961] tortuosity models are expected to perform well for sands (since they were derived assuming randomly distributed particles of equal size) while Modrup's tortuosity models are expected to perform better across soil types.

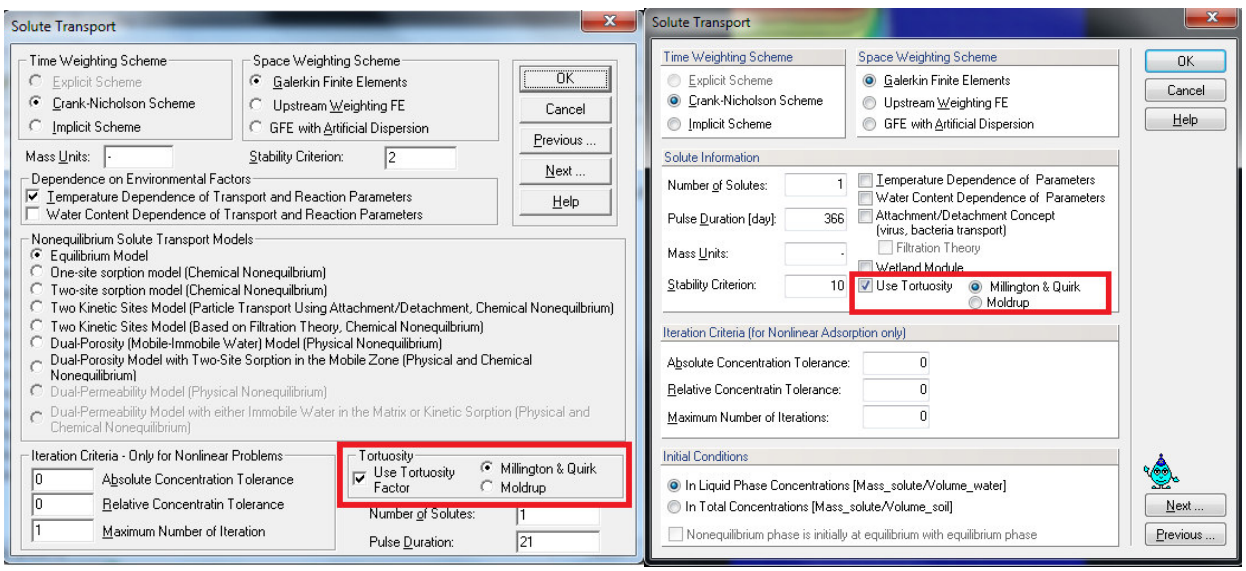

6. Application of a Fumigant at a Specified Time and Location

Fumigants can be applied during the simulation at a selected time using the Fumigant.in input file (see Appendix B at the end of this report), which needs to be placed in the project folder. For this option to become active, both lFumig (activate the transport of fumigants) and lAddF (application of fumigants during the simulation) variables have to be set to .true.. One needs to additionally specify the time when a fumigant is applied (tAddF [T]), the mass of the applied fumigant (FumMass, in [$M_cL_s^{-2}$] or [$M_cL_s^{-1}$] in HYDRUS-1D and HYDRUS (2D/3D), respectively), and the location of fumigant application. In HYDRUS-1D one needs to specify the upper (zAddFT) and lower (zAddFB) depths of the application, in HYDRUS (2D/3D) one needs to specify the upper (zAddFT) and lower (zAddFB) depths and the left (zAddFL) and right (zAddFR) sides of the application. HYDRUS then analyses water and air contents in a particular domain and specifies such a liquid concentration so that the total applied mass corresponds with the specified application mass (FumMass). Any existing mass of fumigant present in the soil profile during the new application is taken into account during these calculations.

7. Two Different Volatilization Boundary Conditions at the Soil Surface

Two different volatilization boundary conditions (as in the figure below)

tarped beds, boundary layer $d = d$(Temp)

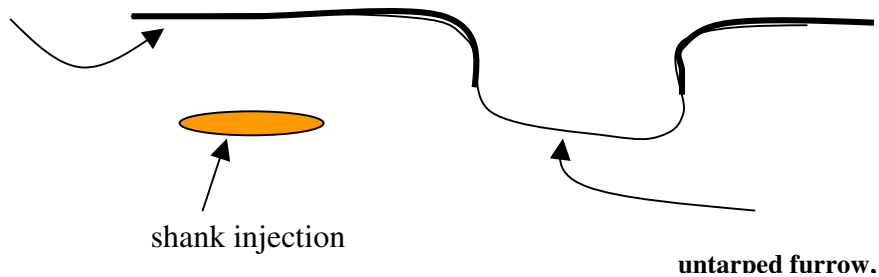

untarped furrow. boundary layer d =0.5 cm

can be used in the new version of HYDRUS (2D/3D) as follows. One needs to use the "Special Boundary Conditions Options", which allow the "Time-Variable Flux 1" boundary to be treated the same way as the "Atmospheric" boundary (in terms of water flow) (checkbox "treat the time-variable flux boundary condition as atmospheric, i.e., with limited pressure heads).

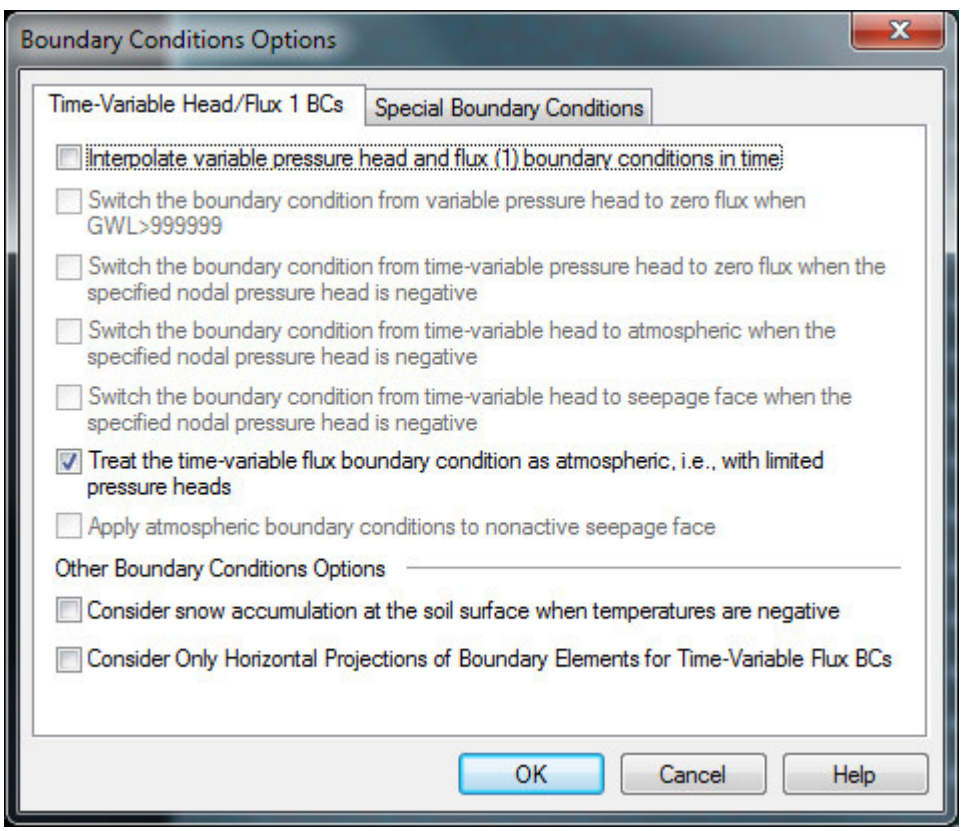

Using this option one can have two separate boundary conditions at the soil surface, which are both treated as Atmospheric boundaries. These two boundaries on the surface can then have either the same or different fluxes, but they are both treated as Atmospheric boundaries. User can apply the "Volatile BC" for solute transport on both of them, and treat the one part (the Atmospheric boundary) as having the tarp, and the second part (the Time-Variable Flux 1 boundary) as not having the tarp (i.e., with d=0.5 cm).

8. References:

Jury, W. A., W. F. Spencer, and W. J. Farmer, Behavior assessment model for trace organics in soil, I. Model description, *J. Environ. Qual., 12*, 558-564, 1983.

Millington, R. J., and J. M. Quirk, Permeability of porous solids, *Trans. Faraday Soc., 57*, 1200-1207, 1961.

Moldrup, P., T. Olesen, D. E. Rolston, and T. Yamaguchi, Modeling diffusion and reaction in soils: VII. Predicting gas and ion diffusivity in undisturbed and sieved soils, *Soil Sci.*, *162*(9), 632-640, 1997.

Moldrup, P., T. Olesen, J. Gamst, P. Schjønning, T. Yamaguchi, and D. E. Rolston, Predicting the gas diffusion coefficient in repacked soil: water-induced linear reduction model, *Soil Sci. Soc. Am. J.*, *64*, 1588-1594, 2000.

Šimůnek, J., M. Th. van Genuchten, and M. Šejna, The HYDRUS-1D software package for simulating the one-dimensional movement of water, heat, and multiple solutes in variably-saturated media. Version 3.0, *HYDRUS Software Series 1*, Department of Environmental Sciences, University of California Riverside, Riverside, CA, 270 pp., 2005.

Šimůnek, J., M. Th. van Genuchten, and M. Šejna, The HYDRUS Software Package for Simulating Two- and Three-Dimensional Movement of Water, Heat, and Multiple Solutes in Variably-Saturated Media, Technical Manual, Version 1.0, PC Progress, Prague, Czech Republic, pp. 241, 2006a.

Šimůnek, J., M. Šejna, and M. Th. van Genuchten, The HYDRUS Software Package for Simulating Two- and Three-Dimensional Movement of Water, Heat, and Multiple Solutes in Variably-Saturated Media, User Manual, Version 1.0, PC Progress, Prague, Czech Republic, pp. 161, 2006b.

Stumm, W., and J. J. Morgan, *Aquatic Chemistry: An Introduction Emphasizing Chemical Equilibria in Natural Waters*, John Wiley & Sons, New York, NY, 1981.

Werner, D., P. Grathwohl, and P. Höhener, Review of field methods for the determination of the tortuosity and effective gas-phase diffusivity in the vadose zone, *Vadose Zone J.*, *3*, 1240-1248, 2004.

9. HYDRUS-1D and HYDRUS (2D/3D) Test Examples

HYDRUS-1D examples:
HYDRUS-1D examples that were used during the HYDRUS course in Sacramento in June 2008 were expanded to demonstrate new capabilities. Currently, there are the following HYDRUS-1D examples of increasing complexity.

Name	Description
Fumig1	No tarp, the initial condition given in liquid concentrations *c*
Fumig1a	No tarp, the initial condition given in total concentrations *S*
Fumig2	Surface tarp, the initial condition given in liquid concentrations *c*
Fumig3	No tarp, the initial condition given in liquid concentrations *c*, irrigation
Fumig4	No tarp, the initial condition given in liquid concentrations *c*, heat transport, effects of temperature
Fumig4a	Surface tarp, the initial condition given in liquid concentrations *c*, heat transport, effects of temperature
Fumig5	Surface tarp removed at a certain time, the initial condition given in liquid concentrations *c*, heat transport, effects of temperature
Fumig6	Surface tarp removed at a certain time, initially no fumigant in the soil profile, heat transport, effects of temperature, fumigant applied at a certain time
Fumig6a	Surface tarp removed at a certain time, the initial condition given in liquid concentrations *c*, heat transport, effects of temperature, fumigant applied at a certain time (i.e., two applications - initially and at a certain time).

HYDRUS-2D examples:
HYDRUS (2D/3D) two-dimensional examples that were used during the HYDRUS course in Sacramento in June 2008 were expanded to demonstrate new capabilities. Currently, there are the following two-dimensional HYDRUS examples of increasing complexity.

Name	Description
Fumig1	Impermeable tarp (infinite resistance), the initial condition given in liquid concentrations *c*
Fumig2	No tarp (no resistance), the initial condition given in liquid concentrations *c*
Fumig3	Surface tarp (finite resistance), the initial condition given in liquid concentrations *c*
Fumig4	No tarp (no resistance), the initial condition given in liquid concentrations *c*, surface irrigation
Fumig5	Surface tarp removed at a certain time, the initial condition given in liquid concentrations *c*, heat transport, effects of temperature
Fumig6	Surface tarp removed at a certain time, initially no fumigant in the soil profile, heat transport, effects of temperature, part of the surface is untarped
Fumig7	Surface tarp removed at a certain time, the initial condition given in liquid concentrations *c*, heat transport, effects of temperature, fumigant applied at a certain time (i.e., two applications - initially and at a certain time).

10. The Fumigants.in Input File

The Input file Fumigants.in (in HYDRUS-1D), which initiates several new options for the fumigant transport (tarp removal, fumigant application during simulation) has to be located in the folder with the corresponding project:

```
*** BLOCK X: FUMIGANT INFORMATION ************************************
Fumigants (lFumig)
t
Additional Application (lAddF)
t
Application Time (tAddF)    Additional Mass (FumMass)
7                           7.63
Appl. Top (zAddFT)          Appl.Bottom (zAddFB)
30                          45
*** END OF INPUT FILE 'FUMIGANT.IN' ***********************************
```

lFumig: =t: if new fumigant options are used, i.e., a) tarp removal, b) additional fumigant application, or c) new output files.
=f: if regular HYDRUS is to be used.
lAddF =t: additional fumigant application at a certain time
=f: no additional fumigant application
tAddF time of additional fumigant application [T]
FumMass mass of applied fumigant [$M_cL_s^{-2}$]
zAddFT z-coordinate (positive) of the top of additional fumigant application [L]
zAddFB z-coordinate (positive) of the bottom of additional fumigant application [L]

The Input file Fumigants.in (in HYDRUS (2D/3D)), which initiates several new options for the fumigant transport (tarp removal, fumigant application during simulation) has to be located in the folder with the corresponding project:

```
*** BLOCK X: FUMIGANT INFORMATION ************************************
Fumigants (lFumig)
t
Additional Application (lAddF)
t
Application Time (tAddF)    Additional Mass (FumMass)
7                           7.63
Appl. Left (xAddFL) Appl.Right (xAddFR) Appl. Top (zAddFT) Appl.Bottom (zAddFB)
20                  30                  50                 30
*** END OF INPUT FILE 'FUMIGANT.IN' ***********************************
```

lFumig: =t: if new fumigant options are used, i.e., a) tarp removal, b) additional fumigant application, or c) new output files.
=f: if regular HYDRUS is to be used.
lAddF =t: additional fumigant application at a certain time
=f: no additional fumigant application
tAddF time of additional fumigant application [T]
FumMass mass of applied fumigant [$M_cL_s^{-1}$]
xAddFL x-coordinate of the left side of the zone of additional fumigant application [L]
xAddFR x-coordinate of the right side of the zone of additional fumigant application [L]
zAddFT z-coordinate of the top of additional fumigant application [L]
zAddFB z-coordinate of the bottom of additional fumigant application [L]